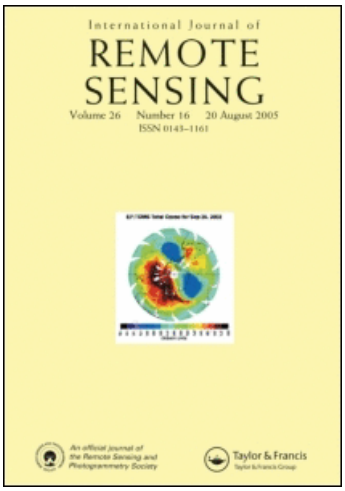

International Journal of Remote Sensing
Publication details, including instructions for authors and subscription information:
http://www.informaworld.com/smpp/title~content=t713722504

Estimation of the gross primary production of an old-growth temperate mixed forest using eddy covariance and remote sensing

J. B. Wu [a]; X. M. Xiao [b]; D. X. Guan [a]; T. T. Shi [a]; C. J. Jin [a]; S. J. Han [a]
[a] Institute of Applied Ecology, Chinese Academy of Sciences, Shenyang 110016, China [b] Institute for the Study of Earth, Oceans and Space, University of New Hampshire, Durham, NH 03824, USA

Online Publication Date: 01 January 2009

To cite this Article Wu, J. B., Xiao, X. M., Guan, D. X., Shi, T. T., Jin, C. J. and Han, S. J.(2009)'Estimation of the gross primary production of an old-growth temperate mixed forest using eddy covariance and remote sensing',International Journal of Remote Sensing,30:2,463 — 479

To link to this Article: DOI: 10.1080/01431160802372143

URL: http://dx.doi.org/10.1080/01431160802372143

International Journal of Remote Sensing
Vol. 30, No. 2, 20 January 2009, 463–479

Taylor & Francis
Taylor & Francis Group

Estimation of the gross primary production of an old-growth temperate mixed forest using eddy covariance and remote sensing

J. B. WU†, X. M. XIAO‡, D. X. GUAN*†, T. T. SHI†, C. J. JIN† and S. J. HAN†

†Institute of Applied Ecology, Chinese Academy of Sciences, Shenyang 110016, China
‡Institute for the Study of Earth, Oceans and Space, University of New Hampshire, Durham, NH 03824, USA

(*Received 18 April 2007; in final form 2 July 2008*)

Continuous flux data from CO_2 flux sites can be used to improve our understanding of leaf phenology and validate the algorithms of satellite- based carbon cycling models. In this study, we conducted a simulation of the Vegetation Photosynthesis Model (VPM) using the Enhanced Vegetation Index (EVI) and the Land Surface Water Index (LSWI) derived from the 8-day Moderate Resolution Imaging Spectroradiometer (MODIS) surface reflectance product, as well as site-specific air temperature, biological temperature, and photosynthetically active radiation (PAR) data. Gross primary production (GPP) estimates derived from the VPM were compared with field observations of a flux tower in an old temperate mixed forest in northeastern China during 2003–2005. Time series data for the EVI have a stronger exponential relationship with the GPP (R^2=0.74, n=67, p<0.01) than those for the Normalized Difference Vegetation Index (NDVI) (R^2=0.62, n=67, p<0.01), indicating a different light use efficiency during the different stages of foliage development. In comparison to the flux tower GPP, the VPM-predicted GPP captured the onset of the growing season well, and their seasonal dynamics were generally consistent in terms of phase in the peak growing season, while the end date of the growing season was 8–16 days earlier than that of field measurements. The annual forest GPP estimated from the flux tower observations varied from 1312 g C m^{-2} (grams of carbon per metre squared) to 1490 g C m^{-2} in the three observation years from 2003 to 2005, which is less 10% different from the VPM-based annual GPP. These results demonstrate the potential of the satellite-driven VPM for scaling up the GPP of forests at the CO_2 flux tower site, a key issue for the study of the carbon budget at regional scales.

1. Introduction

The gross primary production (GPP) of vegetation is one of the key elements that determine the strength of the carbon sink for a terrestrial ecosystem. For decades, numerous methods were used to estimate the GPP; these were mostly process-based biogeochemical models based on a structural perspective of the vegetation canopy. These models use the leaf area index (LAI) or the fraction of incident photosynthetically active radiation (PAR) absorbed by the vegetation canopy ($FPAR_{canopy}$) as a scalar. With the development of satellite remote sensing technology to characterize vegetation structure, scientists sought to develop

*Corresponding author. Email: bjfu_1999@hotmail.com

International Journal of Remote Sensing
ISSN 0143-1161 print/ISSN 1366-5901 online
http://www.tandf.co.uk/journals
DOI: 10.1080/01431160802372143

applicable models formulated from empirical relationships with remote sensing data to estimate the GPP for forest areas (Ruimy *et al.* 1999, Running *et al.* 2000). Several satellite-based modelling studies (e.g. Prince and Goward 1995, Behrenfeld *et al.* 2001, Turner *et al.* 2003) have used the Production Efficiency Model (PEM) to estimate the GPP at large spatial scales:

$$\mathrm{GPP} = \varepsilon_g \times \left(\mathrm{FPAR}_{\mathrm{canopy}}\right) \times (\mathrm{PAR}) \quad (1)$$

where ε_g is the light use efficiency. In these PEMs, $\mathrm{FPAR}_{\mathrm{canopy}}$ is estimated as a simple linear function of a greenness-related vegetation index, the Normalized Difference Vegetation Index (NDVI; Myneni and Williams 1994), while the NDVI is calculated from surface reflectance in the red and near-infrared (NIR) spectral bands (Tucker 1979). The simplicity of the NDVI and its inherent link to photosynthetic activity make it a powerful tool for deriving empirical relationships between $\mathrm{FPAR}_{\mathrm{canopy}}$ and the GPP, and it has been widely used in PEMs (Prince and Goward 1995). However, application of these empirical NDVI models is limited to the regions and time frames for which the regression equations were formulated. In addition, these regression models have to be re-evaluated each season, which limits their practical utility.

In 1999, the Moderate Resolution Imaging Spectroradiometer (MODIS) sensor onboard the National Aeronautics and Space Administration (NASA) Terra satellite was launched. This new sensor allows scientists to gauge the GPP of global terrestrial vegetation on a daily basis. It helps scientists to refine various models to simulate how the land biosphere influences the natural cycles of carbon, water and energy throughout the terrestrial ecosystems. The standard MODIS-based GPP products generated at 1-km spatial resolution are now available to the public (Running *et al.* 2004).

At the same time, remote sensing GPP validation efforts are being conducted globally (Turner *et al.* 2005, Heinsch *et al.* 2006, Coops *et al.* 2007), especially at sites of FLUXNET (Wylie *et al.* 2003), a global network of tower sites that use eddy covariance techniques to continually measure the exchange of CO_2 and water vapour between terrestrial ecosystems and the atmosphere. Because of its high precision and high resolution, the eddy covariance technique based on turbulence theory has emerged as an important tool for evaluating fluxes of mass and energy between vegetation and the atmosphere. CO_2 flux measurements at individual CO_2 eddy flux sites provide abundant and valuable datasets at different time steps, offering new opportunities to examine daily, seasonal and multiyear dynamics of the GPP at stand and ecosystem scales. The eddy covariance method provides information that helps to validate carbon assimilations being determined using remote sensing method.

Recent work by Xiao *et al.* (2004*a*,*b*, 2005*a*,*b*) describes the development of a satellite-based Vegetation Photosynthesis Model (VPM). This model considers vegetation canopy structure from the biochemical perspective with a focus on leaf chlorophyll and leaf water content as well as the fraction of PAR absorbed by chlorophyll ($\mathrm{FPAR}_{\mathrm{CHI}}$). It estimates $\mathrm{FPAR}_{\mathrm{CHI}}$ by using the Enhanced Vegetation Index (EVI). The Land Surface Water Index (LSWI) related to leaf water content and soil moisture was introduced to indicate the effect of water on photosynthesis. The effect of leaf age (from leaf bud to full leaf expansion) on photosynthesis for deciduous species was also considered. The VPM offers a new approach to scale up photosynthesis directly from leaves to ecosystem levels, and it has been evaluated at

some CO_2 eddy flux tower sites with a variety of ecosystem types (e.g. Xiao *et al.* 2005*a*,*b*).

The mixed broadleaved–pine forest in the Changbai Mountain region is an old-growth forest aged about 300 years, with the oldest tree being at least 450 years old according to the tree-ring records (Guan *et al.* 2006). There are only a few such old-growth mixed wood stands even in the global flux tower networks. Hence, the study on carbon processes and GPP in these old-growth forests will provide information complementary to the global FLUXNET database, as well as being of significance for the interpretation and modelling of regional and global carbon cycling. In this paper, a brief description of the satellite-based VPM is given, and then the model is applied to this old forest site. CO_2 flux data were used to evaluate the biophysical performance of vegetation indices with a focus on leaf phenology (the beginning and ending of the plant growing season). The objective of our study was twofold: (1) to understand the leaf phenology of an old-growth mixed forest from satellite images, and (2) to evaluate VPM-predicted GPP using flux tower GPP. The results will help to validate the dependability of the VPM in estimating the GPP of old-growth forest ecosystems.

2. Materials and methods

2.1 *Description of the CO_2 eddy flux tower site in the Changbai Mountain region, northeast China*

In northeast China (42–46° N, 126–131° E), the forests cover $5.7 \times 10^5\,km^2$ and account for more than 30% of the whole region. The broadleaved–Korean pine mixed forests are typical of the temperate mixed forests in northeast China. The CO_2 eddy flux tower site (42°24′9″ N, 128°5′45″ E, figure 1) in Changbai Mountain is located within the forests and is one of the ChinaFlux network sites. ChinaFlux is an independent regional network of the global FLUXNET network, established in 2002 based on the standard measurement methodology of the FLUXNET. The terrain surrounding the flux tower is flat. The mixed forest stand extends for more than 10 km in the prevailing wind directions.

The flux tower site is in a monsoon-influenced, temperate continental climatic zone, where the annual average temperature is 3.5°C and the annual precipitation is

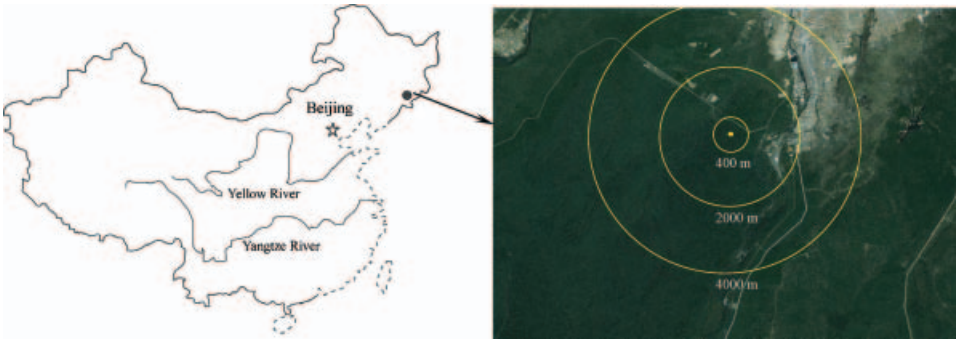

Figure 1. The geographical location of the Changbai Mountain forest flux site (marked with dark circle) and surface cover in the vicinity of the flux tower, in northeast China. The yellow circle in the right panel indicates the location of the flux tower.

713 mm. The surrounding area is vegetated with an approximately 300-year-old mixed stand of Korean pine (*Pinus koraiensis*), Tuan linden (*Tilia amurensis*), larch (*Larix olgensis* var.), Mono maple (*Acer mono*) and other deciduous species interspersed. The mean canopy height is about 26 m. The aboveground stem volume is 380 $m^3 ha^{-1}$, and the stand density is 560 stems ha^{-1} (stem diameter >8 cm). The forest phenology during the measurement period is characterized by a plant-growing season from May to September.

2.2 *Overview of the VPM*

On the basis of the conceptual partitioning of photosynthetically active vegetation (chloroplasts) and non-photosynthetically active vegetation (e.g. stem, branch and cell wall) within a canopy, Xiao *et al.* (2004*a*,*b*, 2005*a*,*b*) developed the satellite-based VPM to estimation GPP over the photosynthetically active period of vegetation. The functions are described as follows:

$$\mathrm{GPP} = \varepsilon_g \times (\mathrm{FPAR_{CHI}}) \times (\mathrm{PAR}) \tag{2}$$

where $\mathrm{FPAR_{CHI}}$ is the fraction of incident PAR (μmol photosynthetic photon flux density, PPFD) absorbed by leaf chlorophyll in the canopy. It is estimated as a linear function of the EVI. ε_g is the light use efficiency (μmol CO_2/μmol PPFD), and varies with the combined effects of temperature, water and plant phenology:

$$\varepsilon_g = \varepsilon_{\max} \times T_{\mathrm{scalar}} \times W_{\mathrm{scalar}} \times P_{\mathrm{scalar}} \tag{3}$$

where $\varepsilon_{\max}$ is the apparent quantum yield or maximum light use efficiency (μmol CO_2/μmol PPFD), and T_{scalar}, W_{scalar} and P_{scalar} are the scalars for the effects of temperature, water and plant phenology on the light use efficiency of vegetation, respectively.

T_{scalar} is estimated by using the equation developed for the terrestrial ecosystem model (Raich *et al.* 1991):

$$T_{scalar} = \frac{(T - T_{\min})(T - T_{\max})}{(T - T_{\min})(T - T_{\max}) - (T - T_{\mathrm{opt}})^2} \tag{4}$$

where T is the site-specific air temperature, and $T_{\max}$, $T_{\min}$ and T_{opt} are the minimum, maximum and optimal temperatures for photosynthetic activities, respectively. Here, $T_{\min}$, T_{opt} and $T_{\max}$ values are set to 0, 20 and 35°C, respectively, based on earlier studies of this old forest (Wu 2003).

W_{scalar} is the indicator of water on plant photosynthesis. Xiao *et al.* (2004*a*) proposed a simple approach that uses a satellite-derived water index to estimate the seasonal dynamics of W_{scalar}:

$$W_{scalar} = \frac{1 + \mathrm{LSWI}}{1 + \mathrm{LSWI_{max}}} \tag{5}$$

where LSWI is the Land Surface Water Index and $\mathrm{LSWI_{max}}$ is the maximum LSWI within the growing season for individual pixels. As the shortwave infrared (SWIR) spectral band is sensitive to vegetation water content and soil moisture, a combination of NIR and SWIR bands has been used to derive water-sensitive vegetation indices (Ceccato *et al.* 2002, Xiao *et al.* 2004*a*). The LSWI was calculated as the normalized difference between the NIR (0.78–0.89 μm) and the SWIR (1.58–1.75 μm) spectral bands of the MODIS sensor:

$$\mathrm{LSWI} = \frac{\rho_{\mathrm{NIR}} - \rho_{\mathrm{SWIR}}}{\rho_{\mathrm{NIR}} + \rho_{\mathrm{SWIR}}} \tag{6}$$

where ρ_{NIR} and ρ_{SWIR} are reflectance data of the NIR and SWIR bands, respectively.

P_{scalar} is defined by vegetation type. After full leaf expansion, P_{scalar} is set to 1.

$$P_{\mathrm{scalar}} = (1 + \mathrm{LSWI})/2 \tag{7}$$

The input data of the VPM model are the EVI, the LSWI, the air temperature T and the PAR. The EVI and LSWI are derived from remote sensing data and are the two vegetation indices that characterize the growing conditions of the vegetation.

The EVI equation takes the form:

$$\mathrm{EVI} = G \times \frac{\rho_{\mathrm{NIR}} - \rho_{\mathrm{red}}}{\rho_{\mathrm{NIR}} + C_1\,\rho_{\mathrm{red}} - C_2 \times \rho_{\mathrm{blue}} + L} \tag{8}$$

where ρ_{blue} and ρ_{red} are reflectance data for the blue and red bands, respectively, L is the canopy background adjustment term, and C_1 and C_2 are the coefficients of the aerosol resistance term, which uses the blue band to correct for aerosol influences in the red band. The coefficients adopted in the EVI algorithm are: $L=1$, $C_1=6$, $C_2=7.5$ and G (gain factor)$=2.5$ (Huete *et al.* 1997).

We conducted a simulation of the VPM using the vegetation indices EVI and LSWI derived from the 8-day MODIS surface reflectance product, site-specific air temperature and biological temperature, and PAR data from the tower site.

2.3 *Description of field data and MODIS image acquisition*

2.3.1 Field data from the CO_2 flux tower site. One set of open-path eddy covariance (EC) systems was mounted on a 62-m tall meteorological tower to measure the Net Ecosystem Exchange (NEE) of CO_2 between the forest and the atmosphere. The sensors were placed on a boom located 40 m (one and half times the average tree height) above the ground and extending 3 m upwind of the tower to minimize flow distortion caused by the tower structure. Wind velocity and virtual temperature fluctuations were measured with a three-dimensional sonic anemometer (CSAT3; Campbell Inc., Logan, UT, USA). CO_2 concentration fluctuations were measured with a fast response open-path, infrared gas analyser (Li7500; Li-cor Inc., Lincoln, NE, USA). The sensor responded to frequencies up to 10 Hz.

Soil temperatures were measured with multilevel thermocouple probes, with sensors placed at 5, 10, 20 and 50 cm below the surface. Soil water content (W_s) was measured concurrently at 5 cm depth using two Time Domain Reflectometry (TDR) probes (CS616; Campbell Inc.). Air temperature was measured with HMP-45C sensors, with sensors placed at 2, 16, 22, 26, 32 and 60 m. The sensors of ancillary measurement responded to frequencies up to 0.5 Hz. To coincide with the flux measurements, 30-min averages were stored in a datalogger (CR5000; Campbell Inc.) and downloaded automatically to a computer. In addition, the LAI was measured above 16 permanent sampling plots, at 5–10-day intervals, using a canopy analyser (Li2000; Li-cor Inc.) along a 200 m transect in a southwesterly direction from the tower during the growing season.

Field measurements of CO_2 flux and climatic parameters at the flux tower site have been recorded since September 2002. Daily GPP values were derived from partitioning of the NEE into the GPP and ecosystem respiration, using the

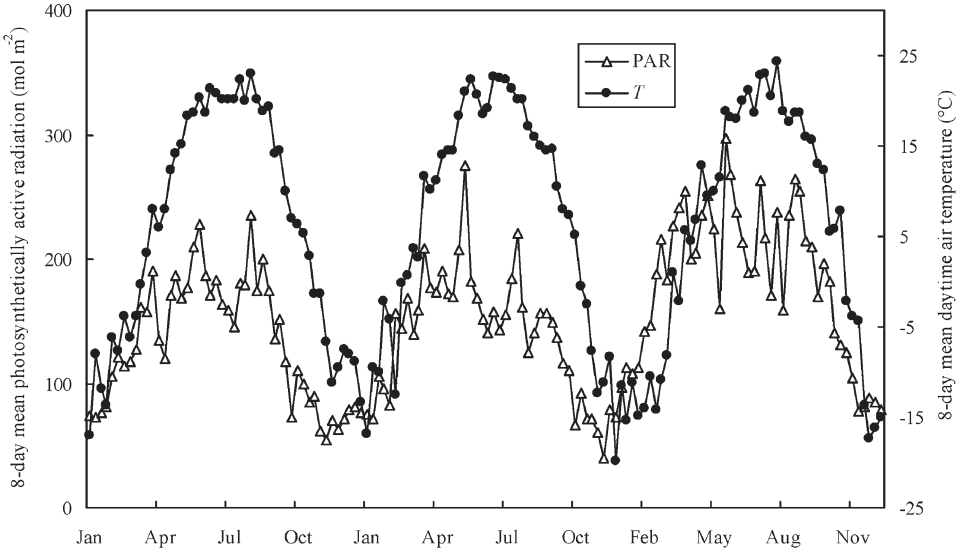

Figure 2. Seasonal dynamics of photosynthetically active radiation (PAR) and mean air temperature (T) during 2003–2005 at the forest flux site in Changbai Mountain, northeast China.

modelling approaches described previously (Wu *et al.* 2006*b*). Daily climate and CO_2 flux data were aggregated to the 8-day interval as defined by the 8-day composite MODIS images, including 8-day sums of PAR and CO_2 flux data, and 8-day means of daytime air temperature (see figure 2).

2.3.2 The 8-day composite images of land surface reflectance from the MODIS sensor. The MODIS sensor acquires daily images of the globe at a spatial resolution of 250 m for red (620–670 nm) and NIR (841–875 nm) bands, and at a spatial resolution of 500 m for blue (459–479 nm), green (545–565 nm), NIR (1230–1250 nm) and SWIR bands (1628–1652 and 2105–2155 nm). The MODIS Land Science Team provides 8-day composite products to the users (http://modis-land.gsfc.nasa.gov/), including the 8-day Land Surface Reflectance product (MOD09A1) that has the above-mentioned spectral bands. We downloaded the 8-day MOD09-A1 data sets for the period of 2003–2005 from the Earth Resources Observation and Science (EROS) Data Center, US Geological Survey (http://edc.usgs.gov/). Reflectance values of the MOD09A1 data set from the four spectral bands blue, red, NIR (841–875 nm) and SWIR (1628–1652 nm) were used to calculate the vegetation indices NDVI, EVI and LSWI. Based on the geolocation information (latitude and longitude) of the CO_2 flux tower site, data for vegetation indices were extracted from one MODIS pixel that is centred on the flux tower.

2.3.3 Estimating maximum light use efficiency. The maximum light use efficiency can be obtained from the canopy-scale quantum yield (α), which represents the initial slope of the relationship between the NEE of CO_2 and the incident photosynthetic photon flux density. It is a parameter used by many biogeochemical carbon cycling models to translate remotely sensed radiation measurements to an estimation of carbon uptake (Ahl *et al.* 2004). The value of α can be obtained from the analysis of the NEE of CO_2 and incident PAR measured from the CO_2 eddy flux tower. A rectangular hyperbola was used to quantify the relationship between NEE

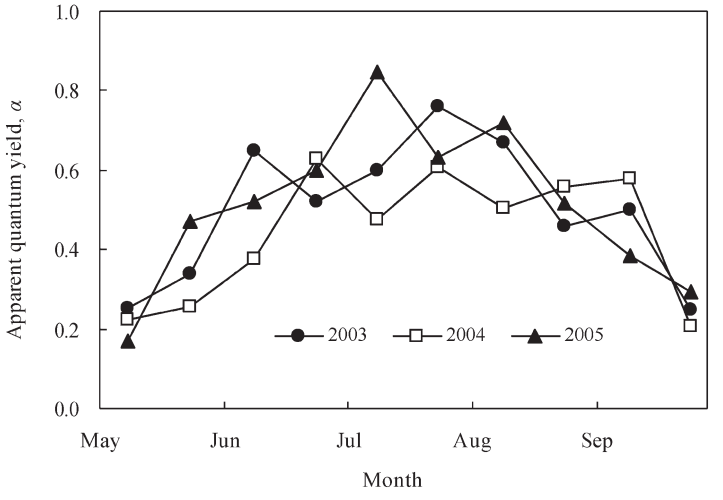

Figure 3. Seasonal evolution of canopy-scale quantum yield during 2003–2005 at the forest flux site in Changbai Mountain, northeast China. α is the apparent quantum yield in units of g C mol^{-1} PAR.

and incoming PAR:

$$\mathrm{NEE} = \frac{\alpha \times \beta \times \mathrm{PAR}}{\alpha \times \mathrm{PAR} + \beta} - R_{\mathrm{e}} \tag{9}$$

where α is the apparent quantum yield or initial slope of the light response curve, β is the value of the NEE at light saturation, and R_{e} is the respiration term. The seasonal and interannual evolution of α is shown in figure 3. The maximum of monthly average α generally appeared in June and July rather than in the month with highest LAI, with values in the range 0.62–0.83 grams of carbon (g C) mol^{-1} PAR. These values are well within the range of reported α values for other forest canopies (α=0.16–0.98 g C mol^{-1} PAR; reviewed by Singsaas *et al.* 2001).

3. Results

3.1 *Seasonal dynamics of the NDVI and EVI from 8-day composites of MODIS*

Seasonal dynamics of the EVI within the growing season at the forest site differed substantially from those of the NDVI in terms of phase and magnitude (figure 4(*a*)). The maximum EVI values in summer were 0.64, 0.66 and 0.67 in the three observational years from 2003 to 2005; these values are much lower than the corresponding maximum NDVI values of 0.90, 0.89 and 0.93. The EVI curve from the MODIS sensor changed significantly over time, reaching its peak in early summer and then declining gradually. It reached a maximum plateau 40 days earlier than the occurrence of maximum LAI and the maximum intercepted fraction of PAR absorbed by the vegetation canopy ($\mathrm{FPAR}_{\mathrm{canopy}}$) derived from *in situ* measurements (figure 4(*b*)). The NDVI exhibited saturated signals when the canopy was full in early June, and responded to canopy structure variation until leaf senescence in mid- September. The NDVI had a maximum temporal plateau for more than 70 days, which nearly covered the full peak-growing season stage. Therefore, the difference between EVI and NDVI was considerable during the peak growing seasons. There is a moderate linear relationship between NDVI and EVI

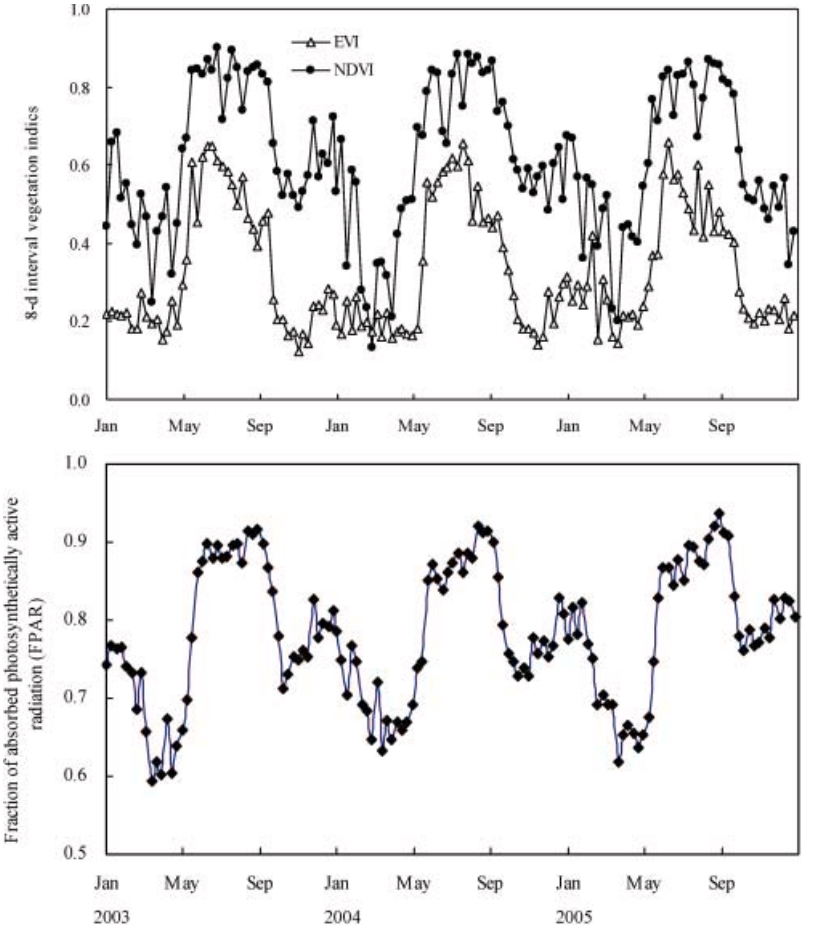

Figure 4. Seasonal dynamics of vegetation indices (EVI and NDVI) and fraction of photosynthetically active radiation absorbed by the vegetation canopy ($FPAR_{canopy}$) during 2003–2005 in forests of Changbai Mountain, northeast China.

(R^2=0.64, n=67) for the total growing seasons of 2003–2005. This may be because the NDVI values were saturated in well-vegetated areas, as the LAI at the old-growth forest site is relatively high (up to 6.0). The EVI does not seem to be as saturated as the NDVI. Thus, the EVI is still sensitive to phenological changes in leaf and canopy. This indicated that the MODIS-based EVI provides more accurate vegetation growing information for plant phenology description than the NDVI, especially for stands with high biomass.

3.2 *Seasonal dynamics of CO_2 fluxes and MODIS data in 2003–2005*

The GPP time series during 2003–2005 for the mixed forest site had a distinct seasonal cycle (figure 5). GPP values were near zero in the winter season (December–March) when the canopy is 'dominated by deciduous trees and the low air temperature inhibits photosynthetic activities of conifers (figure 2). The GPP began to increase in late April and reached its peak in late June to early July. It declined gradually after its peak, even though the LAI hardly changed over the period

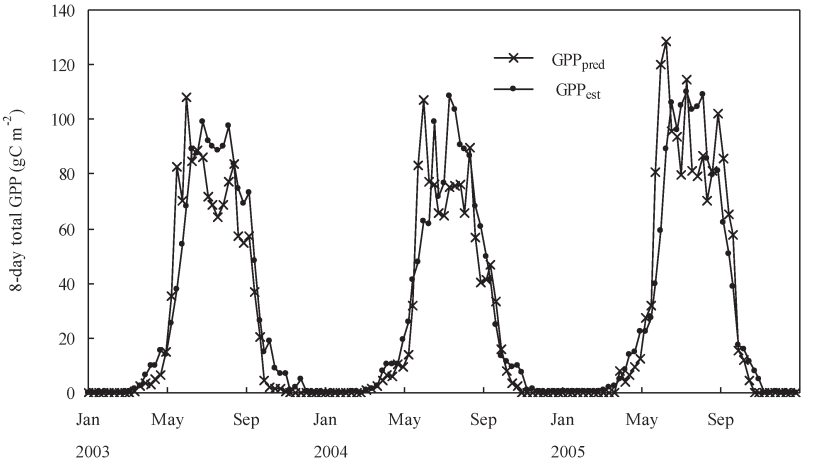

Figure 5. Seasonal dynamics of 8-day gross primary production ($g\,C\,m^{-2}$) at the flux site in Changbai Mountain. The predicted GPP (GPP_{pred}) is from the VPM, using 8-day MODIS composites. The estimated GPP (GPP_{est}) is derived from eddy flux tower observations.

between July and September. The seasonal dynamics of the GPP can be mostly explained by the seasonal variations in air temperature and PAR (Wu *et al.* 2006*a*).

Figure 6 shows the seasonal evolution of the rectangular hyperbolic relationship (see equation (9)) between the daytime NEE of CO_2 and PAR. There are significant correlations ($R^2=0.42$–0.78, $p<0.05$) between net CO_2 assimilatory rates and PAR during the growing season. Although the phenology of the mixed forest is characterized by a growing season from May to September, the data indicate that low carbon assimilation activity also occurred in April, which indicated that the evergreen Korean pine keeps an active photosynthetic capacity before the onset of bud-burst in deciduous species. The forest shows a strong CO_2 assimilation capacity during June and August, with the maximum CO_2 assimilation rates occurs in July, which is consistent with the data shown in figure 5. Seasonally integrated GPP over the period from 1 May to 1 October accounts for 93% (2003), 91% (2004) and 94% (2005) of the annually integrated GPP, respectively.

The time series of LSWI data has a distinct seasonal cycle with low value areas appearing in spring and autumn (figure 7). High LSWI values appeared in late autumn, winter and early spring, during which period the forest site is always covered with snow (above or below the canopy). A snow pack of up to 40 cm could exist from December to March. Snow has much higher reflectance in the visible and NIR bands, in comparison to vegetation. The high LSWI values in winter and early spring are attributed to snow cover in the forest stands. As snow melted in late spring, the LSWI decreased. The 8-day periods that had minimum LSWI values in early spring were 15–22 April 2003, 23–30 April 2004 and 23–30 April 2005. The threshold of the lowest LSWI value in spring corresponds to the beginning of the photosynthetically active period of the evergreen needleleaf forest and early spring herbs. The LSWI increased through spring and reached its peak in early July. The 8-day periods that have a minimum LSWI in autumn were 16–23 October 2003, 24–31 October 2004 and 16–23 October 2005. The threshold of the lowest LSWI value in autumn corresponds to the end of the photosynthetically active period. The troughs of LSWI in the spring and autumn delineate the starting and ending dates of the plant growing season as well as

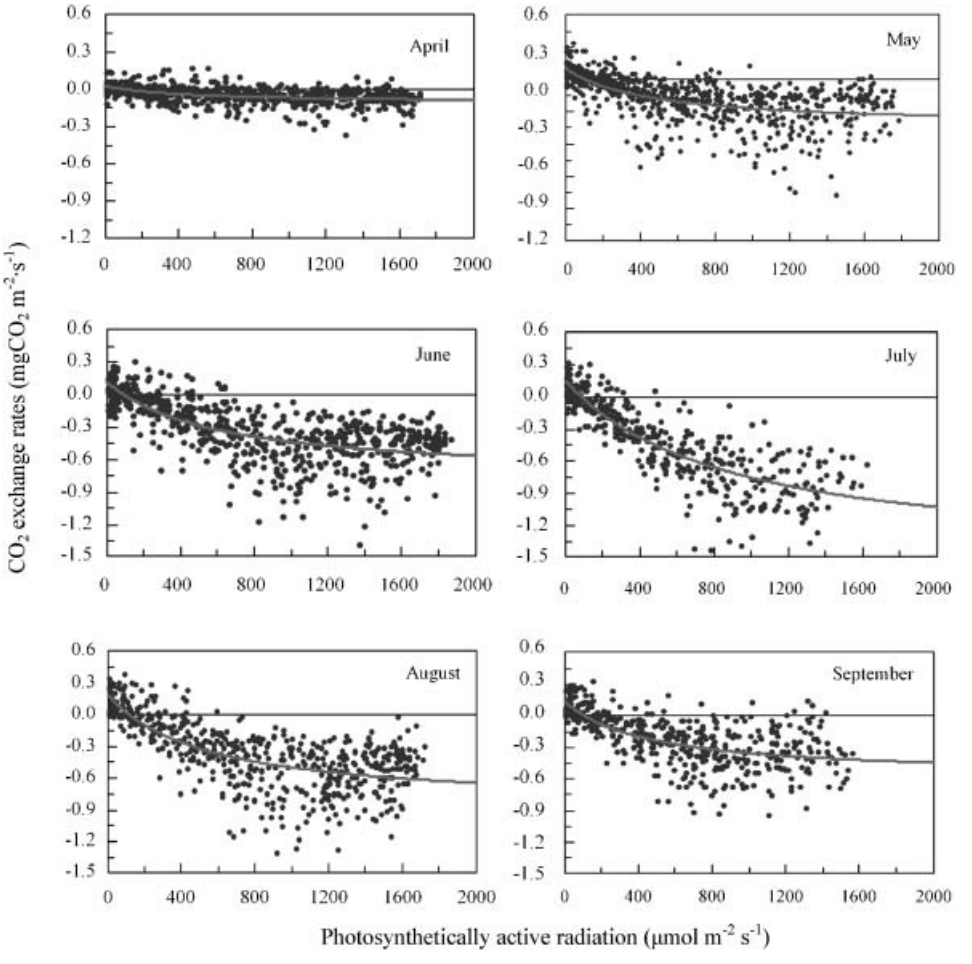

Figure 6. Seasonal variations of net ecosystem CO_2 exchange in response to photosynthetically active radiation (30-min interval in daytime) between the forest and the atmosphere during April–September, at the flux tower site in Changbai Mountain, northeast China.

the length of the plant growing season in this old forest site, which is consistent with observations in other forest types (Xiao *et al.* 2004*b*, 2005*a*).

3.3 *Analyses of the relationships between vegetation indices and the GPP*

For this study, half-hourly observations from the flux tower were aggregated to the 8-day time step. The temporal dynamics of the EVI within the plant-growing season (May to October) correlated closely to the dynamics of the observed GPP at the forest tower sites (see figure 5). Comparisons between vegetation indices (EVI, NDVI) and the GPP have shown that the seasonal dynamics of the EVI was more consistent with those of the GPP in terms of phase (figures 4(*a*) and 5). EVI curves had a peak value in early July, while NDVI curves had a plateau from July to September. Therefore, when using the growing season observations in 2003–2005, the EVI had a stronger exponential relationship ($R^2=0.74$, $n=67$, $p<0.01$) with the eddy flux tower estimates of GPP (GPP_{est}) than NDVI ($R^2=0.62$, $n=67$, $p<0.01$) (figure 8). This indirectly supports the idea that to estimate the remote sensing-based GPP, application of a

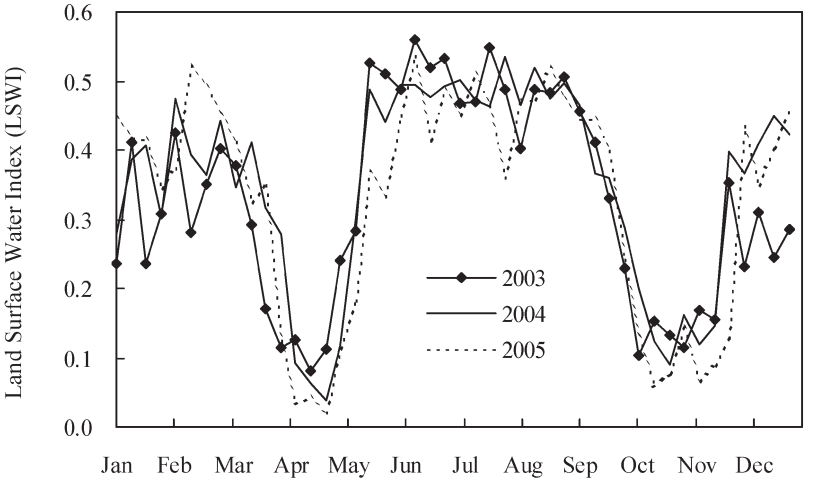

Figure 7. Seasonal dynamics of the Land Surface Water Index (LSWI) during 2003–2005 at the flux site in Changbai Mountain, northeast China.

chlorophyll-related vegetation index for photosynthetically active vegetation is more reasonable than that of a greenness-related vegetation index, especially for an old forest with high biomass. The exponential rather than linear relationships between EVI, NDVI and GPP_{est}, according to the proportion of variance of GPP that is predictable from the regressor, also indicate a different light use efficiency during the different stages of foliage development of the forest, as shown in figure 3.

The VPM-predicted values of GPP (GPP_{pred}) were compared with eddy flux tower estimates of GPP_{est} at the flux site. As figure 9 shows, there is a good linear relationship between GPP_{pred} and GPP_{est} ($R^2=0.64$, $p<0.01$) for the whole growing seasons of 2003–2005. At a temporal resolution of 8 days, GPP_{pred} values were generally higher than GPP_{est} in the early summer, and their seasonal dynamics were consistent in terms of phase in the peak growing season (figures 5 and 9). The annual total GPP_{pred} values were 1312, 1189 and 1477 $g\,C\,m^{-2}$ in the three observation years from 2003 to 2005, values that were slightly lower than the corresponding ones of the flux tower GPP_{est} (1433, 1312 and 1490 $g\,C\,m^{-2}$). This was acceptable because the differences between them were generally less than 10%. It is worth noting that the starting date of the growing season (here the threshold of the growing seasoning was defined as $GPP>0.5\,g\,C\,m^{-2}$) driven from the MODIS GPP was consistent with the ground-based plant growing season, but the end date of the growing season was generally 8–16 days earlier than the ground-based measurement. It is interesting to note that, even in winter when the daily mean air temperature falls below 0°C, the field-observed flux still showed that carbon assimilation occurred at noon at the forest site, as reported also by Sevanto *et al.* (2006) and Wu *et al.* (2006*b*). In the VPM, if the air temperature falls below T_{min}, T_{scalar} is set to be zero, thus the modelled GPP should be zero. Therefore, the end date of the growing season referring to GPP_{pred} values was always earlier than that of the ground-based measurements.

4. Discussion and conclusion

To estimate the ecosystem GPP more precisely, scientists have been developing innovative algorithms and models, taking full advantage of advanced optical

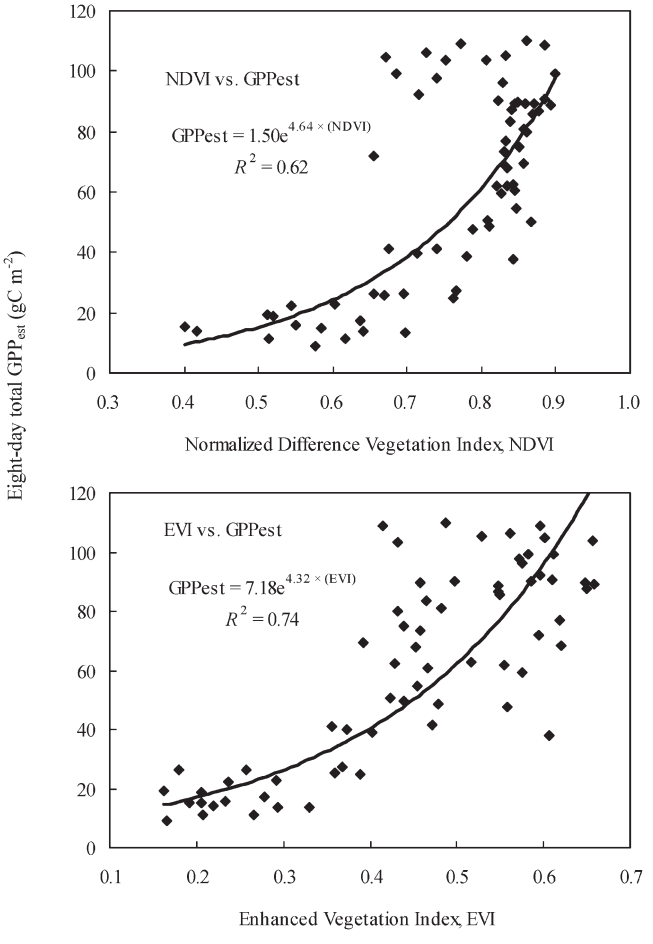

Figure 8. The quantitative relationships between the GPP estimated from the tower measurements and vegetation indices during the plant growing season, from 2003 to 2005, at the flux site in Changbai Mountain, northeast China.

sensors. Remote sensing satellite observation has the capability to retrieve vegetation and climatic parameters with relatively high precision. However, the multiple inputs to the remote sensing GPP algorithm are generally subject to uncertainty and require intensive field validation campaigns. Nowadays, an increasing number of flux tower sites are producing GPP estimates with relevance to validating MODIS products (Baldocchi *et al.* 2001, Falge *et al.* 2002, Wylie *et al.* 2003, Turner *et al.* 2004, Veroustraete *et al.* 2004).

In this study, the satellite-based VPM was applied to an old-growth mixed forest, and the modelling results compared with flux tower-based GPP values. We have shown that whereas the NDVI is sensitive to greenness, the EVI is more responsive to canopy structural variations, including chlorophyll and plant phenology. The annual GPP of the old-growth forest varied between 1312 and 1490 $g C m^{-2}$ based on flux tower measurements from 2003 to 2005. The VPM-predicted GPP tended to be lower than the annual flux tower GPP, but the underestimation was generally no more than 10%. Compared with eddy flux tower observation, the VPM-predicted GPP captures well the onset of the growing

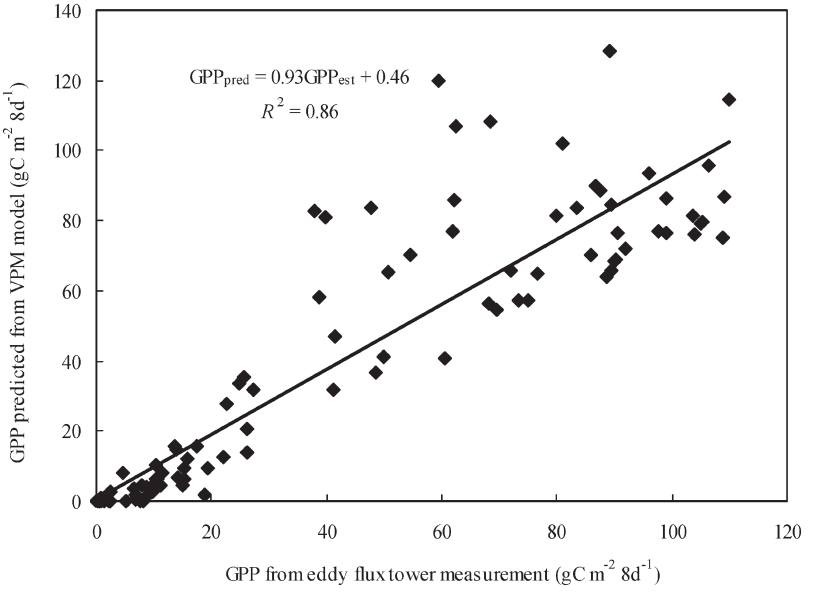

Figure 9. A comparison between VPM-predicted GPP and estimated GPP from tower data at the flux tower site in Changbai Mountain, northeast China.

season, while the end date of growing season was generally 8–16 days earlier than the ground-based measurement.

There are several possible reasons for the differences in the tower and MODIS estimates of the GPP. Turner *et al.* (2006) also reported that the MODIS products tended to be underestimates in high productivity sites, and a similar pattern was found by Heinsch *et al.* (2006) from 15 flux tower sites. The authors pointed out that the underestimations are primarily a function of the relatively low values for the maximum light use efficiency (ε_{max}) that are generated by running the MOD17 GPP algorithm (Running *et al.* 2000). A related issue is that ε_{max} in MOD17 does not respond to overcast conditions, while observations at flux towers suggest that ε_{max} is highest on overcast days and decreases on clear-sky days because of light saturation (Wu *et al.* 2006*a*).

For the current studies, ε_{max} is driven from the tower-based measurement rather than from the MOD17 GPP algorithm. Hence the above flaw can be fixed. Further analysis suggests that there are two other potential causes for the disparity. One is the systematic overestimation of the tower-based GPP. In fact, the prospects for validating the MODIS GPP products are also constrained by uncertainties in the tower-based GPP. Typically it is estimated as the difference between the NEE and the ecosystem respiration (R_e) (e.g. Falge *et al.* 2002, Wu *et al.* 2006*b*), while R_e is scaled either from chamber measurements of soil respiration or from establishing functional relationships between night-time (when photosynthesis is assumed to be zero) NEE and some reference temperature or soil water, above a threshold of friction velocity, and then extrapolated to daytime conditions (e.g. Janssens *et al.* 2001). However, there is one problem associated with this approach, namely the reduction of leaf respiration in light relative to darkness, that causes an overestimation of daytime ecosystem respiration, and then tower-based GPP overestimation may arise from this systematic error. The overestimation was

quantified for a mountain meadow using a coupled model of the reduction of leaf dark respiration, as a function of light intensity and canopy radiative transfer, and suggested overestimation of GPP by 11–17% (Wohlfahrt *et al.* 2005).

In forests, the complexity of canopy structure and radiation environment cause the lack of a realistic assessment of the overestimation of GPP using daytime respiration extrapolated from night-time R_e measurements. The only quantitative estimate of the reduction of GPP available to date is by Janssens *et al.* (2001) for the forests investigated within the EuroFlux project. These authors assert a 15% reduction in canopy respiration in light relative to darkness, but do not elaborate on how this figure was derived. For forest stands with a high biomass of stems and roots, the contribution of leaf respiration to the whole ecosystem is generally less than that of other vegetation. However, it is at least a potential reason accounting for the underlying mechanism of difference between remotes sensing GPP and tower GPP.

Another potential cause for the disparity is issues with mismatches in spatial representative when comparing tower-based GPP with MODIS predictions. Rahman *et al.* (2005) tested the potential of estimating per-pixel GPP directly from the MODIS EVI. The correlation between across-site tower GPP and EVI was comparable (R=0.77) to that between tower GPP and MOD17 GPP (R=0.73), suggesting that the EVI could be used to provide reasonably accurate estimates of the GPP on a simple per-pixel basis, at least for some vegetation types. Because of the relatively high observation platform, the forest flux site generally has a much larger footprint size in comparison with other site types, such as grassland sites. The upwind distance of the flux source area could be at least 1000 m along the streamline directions, which is very similar to MODIS image resolution (250 to 500 m). However, tower-based estimates of GPP depend strongly on wind conditions and atmospheric stability (Schmid 2002). Thus, the tower is sampling over a variable source area surrounding the tower. Given that vegetation composition and age distribution are always heterogeneous in a mixed forest, there is often a difference between the productivity of the remote sensing grid and that of the tower pixel itself. Hence, how to scale-up local measurement of the GPP by the high-resolution EC technique at ground sites to regional scales by remote sensing at more coarse spatial-temporal scalars has always been a challenging issue. To ensure complete validation, multiple measurement strategies such as top-down and bottom-up projects are necessary (Running *et al.* 1999).

The MODIS EVI is an enhanced version of the NDVI and was developed to optimize the vegetation signal with improved sensitivity in high biomass regions, while correcting for canopy background signals and reducing atmosphere influences. Fensholt and Sandholt (2005) reported that the MODIS EVI is more sensitive to dense vegetation than the NDVI, as has been proved in this old-growth forest case. As shown in figure 4(*a*), the NDVI exhibited saturated trends when the canopy was full, and responded to canopy structure variations until leaf senescence, while the EVI presented a clear seasonal change with tree phenology, and non-saturation of EVI has occurred over maximum vegetation density. This suggests that the EVI has more biological significance in GPP predictions than the NDVI. The EVI-based VPM could capture the overall trends of the old-growth mixed forest phenology and provide a reasonable estimation of GPP. The simulation results of the VPM have shown that the predicted GPP agrees well with the observed GPP of the old-growth mixed forest in Changbai Mountain. The results from this study and other studies of an evergreen needleleaf forest (Xiao *et al.* 2004*a*), a deciduous

broadleaf forest (Xiao *et al.* 2004*b*) and even an alpine shrub/meadow (Li *et al.* 2007) demonstrate the potential of the satellite-driven VPM for scaling up the GPP at the CO_2 flux tower sites, a key issue for the study of the carbon budget at regional and global scales.

Acknowledgements

This work was supported by the National Natural Science Foundation of China (40675069, 30700085) and the Special Foundation of President scholarship of CAS. X.M.X. is supported by the NASA Land Cover and Land Use Change Program (NAG5-11160, NNG05GH80G) and the International Partnership Project of Chinese Academy of Sciences (Grant No. CXTD-Z2005-1). We thank the anonymous reviewers for their valuable comments and suggestions.

References

Ahl, D.E., Gower, S.T., Mackay, D.S., Burrows, S.N., Norman, J.M. and Diak, G.R., 2004, Heterogeneity of light use efficiency in a northern Wisconsin forest: implications for modeling net primary production with remote sensing. *Remote Sensing of Environment*, **93**, pp. 168–178.

Baldocchi, D., Falge, E., Gu, L.H., Olson, R., Hollinger, D., Running, S., Anthoni, P., Bernhofer, C., Davis, K., Evans, R., Fuentes, J., Goldstein, A., Katul, G., Law, B., Lee, X.H., Malhi, Y., Meyers, T., Munger, W., Pilegaard, K., Schmid, H.P., Valentini, R., Verma, S., Wilson, K. and Wofsy, S., 2001, FLUXNET: a new tool to study the temporal and spatial variability of ecosystem-scale carbon dioxide, water vapor, and energy flux densities. *Bulletin of the American Meteorological Society*, **82**, pp. 2415–2434.

Behrenfeld, M.J., Randerson, J.T., McClain, C.R., Feldman, G.S., Los, S.O., Tucker, C.J., Falkowski, P.G., Field, C.B., Frouin, R., Esaias, W.E., Kolber, D.D. and Pollack, N.H., 2001, Biospheric primary production during an ENSO transition. *Science*, **291**, pp. 2594–2597.

Ceccato, P., Gobron, N., Flasse, S., Pinty, B. and Tarantola, S., 2002, Designing a spectral index to estimate vegetation water content from remote sensing data: Part 1. Theoretical approach. *Remote Sensing of Environment*, **82**, pp. 188–197.

Coops, N.C., Black, T.A., Jassal, R.S., Trofymow, J.A. and Morgenstern, K., 2007, Comparison of MODIS, eddy covariance determined and physiologically modelled gross primary production in a Douglas-fir forest stand. *Remote Sensing of Environment*, **107**, pp. 385–401.

Falge, E., Baldocchi, D., Tenhunen, J., Aubinet, M., Bakwin, P., Berbigier, P., Bernhofer, C., Burba, G., Clement, R., Davis, K.J., Elbers, J.A., Goldstein, A.H., Grelle, A., Granier, A., Hollinger, D., Kowalski, A.S., Katul, G., Law, B.E., Malhi, Y., Meyers, T., Monson, R.K., Munger, J.W., Oechel, W., Paw, K.T., Pilegaard, U.K., Rannik, U., Suyker, A., Valentini, R., Wilson, K. and Wofsy, S., 2002, Seasonality of ecosystem respiration and gross primary production as derived from FLUXNET measurements. *Agricultural and Forest Meteorology*, **113**, pp. 53–74.

Fensholt, R. and Sandholt, I., 2005, Evaluation of the MODIS and NOAA AVHRR vegetation indices with in situ measurements in a semi-arid environment. *International Journal of Remote Sensing*, **26**, pp. 2561–2594.

Guan, D.X., Wu, J.B., Zhao, X.S., Han, S.J., Yu, G.R. and Jin, C.J., 2006, CO_2 flux over old temperate mixed forest in north-eastern China. *Agricultural and Forest Meteorology*, **137**, pp. 138–149.

Heinsch, F.A., Zhao, M., Running, S.W., Kimball, J.S., Nemani, R.R., Davis, K.J., Bolstad, P.V., Cook, B.D., Desai, A.R., Ricciuto, D.M., Lwa, B.E., Oechel, W.C., Kwon, H.J., Luo, H., Wofsy, S.C., Dunn, A.L., Munger, J.W.,

Baldocchi, D.D., Xu, L., Hollinger, D.Y., Richardson, A.D., Stoy, P.C., Siqueira, M.B.S., Monson, R.K., Burns, S.P. and Flanagan, L.B., 2006, Evaluation of remote sensing based terrestrial productivity from MODIS using regional tower eddy flux network observations. *IEEE Transactions on Geoscience and Remote Sensing*, **44**, pp. 1908–1925.

Huete, A.R., Liu, H.Q., Batchily, K. and Leeuwen, W., 1997, A comparison of vegetation indices over a global set of TM images. *Remote Sensing of Environment*, **59**, pp. 440–451.

Janssens, I.A., Lankreijer, H., Matteucci, G., Kowalski, A.S., Buchmann, N., Epron, D., Pilgeaard, K., Kutsch, W., Longdoz, B., Grunwald, T., Montagnani, L., Dore, S., Rebmannn, C., Moors, E.J., Grelle, A., Rannik, U., Morgenstern, K., Oltchev, S., Clement, R., Gudmundsson, J., Minerbi, S., Berbigier, P., Ibrom, A., Moncrieff, J., Aubinet, M., Bernhofer, C., Jensen, O., Vesala, T., Granier, A., Lindroth, A., Dolman, A.J., Jarvis, P.G., Ceulemans, R. and Valentini, R., 2001, Productivity overshadows temperature in determining soil and ecosystem respiration across European forests. *Global Change Biology*, **7**, pp. 269–278.

Li, Z.Q., Yu, Q.R., Xiao, X.M., Li, Y.N., Zhao, X.Q., Ren, C.Y., Zhang, L.M. and Fu, Y.L., 2007, Modeling gross primary production of alpine ecosystems in the Tibetan Plateau using MODIS images and climate data. *Remote Sensing of Environment*, **107**, pp. 510–519.

Myneni, R.B. and Williams, D.L., 1994, On the relationship between FAPAR and NDVI. *Remote Sensing of Environment*, **49**, pp. 200–211.

Prince, S.D. and Goward, S.N., 1995, Global primary production: a remote sensing approach. *Journal of Biogeography*, **22**, pp. 815–835.

Rahman, A.F., Sims, D.A., Cordova, V.D. and El-Masri, B.Z., 2005, Potential of MODIS EVI and surface temperature for directly estimating per-pixel ecosystem C fluxes. *Geophysical Research Letters*, **32**, pp. L19404, doi:10.1029/2005GL024127.

Raich, J.W., Rastetter, E.B., Melillo, J.M., Kicklighter, D.W., Steudler, P.A., Peterson, B.J., Grace, A.L., Moore, B. and Vorosmarty, C.J., 1991, Potential net primary productivity in South America: application of a global model. *Ecological Applications*, **1**, pp. 399–429.

Ruimy, A., Kergoat, L. and Bondeau, A., 1999, Comparing global models of terrestrial net primary productivity (NPP): analysis of differences in light absorption and light-use efficiency. *Global Change Biology*, **5**(Suppl. 1), pp. 56–64.

Running, S.W., Baldocchi, D.D. and Turner, D.P., 1999, A global terrestrial monitoring network integrating tower fluxes, flask sampling, ecosystem modeling and EOS satellite data. *Remote Sensing of Environment*, **70**, pp. 108–127.

Running, S.W., Nemani, R.R., Heinsch, F.A., Zhao, M., Reeves, M.C. and Hashimoto, H., 2004, A continuous satellite-derived measure of global terrestrial primary production. *BioScience*, **54**, pp. 547–560.

Running, S.W., Thornton, P.E., Nemani, R.R. and Glassy, J.M., 2000, Global terrestrial gross and net primary productivity from the Earth Observing System. In *Methods in Ecosystem Science*, O.E. Sala, R.B. Jackson, E.P. Odum and H.A. Mooney (Eds), pp. 44–57 (New York: Springer).

Schmid, H.P., 2002, Footprint modeling for vegetation atmosphere exchange studies: a review and perspective. *Agricultural and Forest Meteorology*, **113**, pp. 159–183.

Sevanto, S., Suni, T., Pumpanen, J., Gronholm, T., Kolari, P., Nikinmaa, E., Hari, P. and Vesala, T., 2006, Wintertime photosynthesis and water uptake in a boreal forest. *Tree Physiology*, **26**, pp. 749–757.

Singsaas, E.L., Oor, D.R. and de Lucia, E.H., 2001, Variation in measured values of photosynthetic quantum yield in ecophysiological studies. *Oecologia*, **128**, pp. 15–23.

Tucker, C.J., 1979, Red and photographic infrared linear combinations for monitoring vegetation. *Remote Sensing of Environment*, **8**, pp. 127–150.

TURNER, D.P., OLLINGER, S., SMITH, M.L., KRANKINA, O. and GREGORY, M., 2004, Scaling net primary production to a MODIS footprint in support of Earth Observing System product validation. *International Journal of Remote Sensing*, **25**, pp. 1961–1979.

TURNER, D.P., RITTS, W.D., COHEN, W.B., GOWER, S.T., RUNNING, S.W., ZHAO, M., COSTA, M.H., KIRSCHBAUM, A., HAM, J., SALESKA, S. and AHL, D.E., 2006, Evaluation of MODIS NPP and GPP products across multiple biomes. *Remote Sensing of Environment*, **102**, pp. 282–292.

TURNER, D.P., RITTS, W.D., COHEN, W.B., GOWER, S.T., ZHAO, M.S., RUNNING, S.W., WOFSY, S.C., DUNN, A.L. and MUNGER, J.W., 2003, Scaling gross primary production (GPP) over boreal and deciduous forest landscapes in support of MODIS GPP product validation. *Remote Sensing of Environment*, **88**, pp. 256–270.

TURNER, D.P., RITTS, W.D., COHEN, W.B., MAEIRSPERGER, T.K., GOWER, S.T., KIRSCHBAUM, A.A., RUNNING, W., ZHAO, M., WOFSY, S.C., DUNN, A.L., LAW, B.E., CAMPBELL, J.L., OECHEL, W.C., KWON, H., MEYERS, T.P., SMALL, E.E., KURC, S.A. and GAMON, J.A., 2005, Site-level evaluation of satellite-based global terrestrial gross primary production and net primary production monitoring. *Global Change Biology*, **11**, pp. 666–684.

VEROUSTRAETE, F., SABBE, H., RASSE, D.P. and BERTELS, L., 2004, Carbon mass fluxes of forests in Belgium determined with low resolution optical sensors. *International Journal of Remote Sensing*, **25**, pp. 769–792.

WOHLFAHRT, G., BAHN, M., HASLWANTER, A., NEWESELY, C. and CERNUSCA, A., 2005, Estimation of daytime ecosystem respiration to determine gross primary production of a mountain meadow. *Agricultural and Forest Meteorology*, **130**, pp. 13–25.

WU, J.B., GUAN, D.X., SUN, X.M., ZHANG, M., SHI, T.T., HAN, S.J. and JIN, C.J., 2006a, Photosynthetic characteristics of dominant tree species and canopy in the broadleaved Korean pine forest of Changbai Mountain. *Science in China: Series D*, **49**, pp. 89–96.

WU, J.B., GUAN, D.X. and WANG, M., 2006b, Year-round soil and ecosystem respiration in a temperate broad-leaved Korean Pine forest. *Forest Ecology and Management*, **233**, pp. 35–44.

WU, Z.F., 2003, Assessment of eco-climate suitability and climate change impacts of broadleaved Korean pine forest in northeast China. *Chinese Journal of Applied Ecology*, **14**, pp. 771–775.

WYLIE, B.K., JOHNSON, D.A., LACA, E., SALIENDRA, N.Z., GILMANOVD, G.T., REEDA, B.C., TIESZENE, L.L. and WORSTELL, B.B., 2003, Calibration of remotely sensed, coarse resolution NDVI to CO_2 fluxes in a sagebrush–steppe ecosystem. *Remote Sensing of Environment*, **85**, pp. 243–255.

XIAO, X., HOLLINGER, D., ABER, J., GOLTZ, M., DAVIDSON, E.A., ZHANG, Q. and MOORE, B., 2004a, Satellite-based modeling of gross primary production in an evergreen needleleaf forest. *Remote Sensing of Environment*, **89**, pp. 519–534.

XIAO, X., ZHANG, Q., BRASWELL, B., UUBANSKI, S., BOLES, S., WOFSY, S., MOORE, B. and OJIMA, D., 2004b, Modeling gross primary production of deciduous broadleaf forest using satellite images and climate data. *Remote Sensing of Environment*, **91**, pp. 256–270.

XIAO, X., ZHANG, Q., HOLLINGER, D., ABER, J. and MOORE, B., 2005a, Modeling seasonal dynamics of gross primary production of evergreen needleleaf forest using MODIS images and climate data. *Ecological Applications*, **15**, pp. 954–969.

XIAO, X., ZHANG, Q., SALESKA, S., HUTYRA, L., DE CAMARGO, P., WOFSY, S., FROLKING, S., BOLES, S., KELLER, M. and MOORE, B., 2005b, Satellite-based modeling of gross primary production in a seasonally moist tropical evergreen forest. *Remote Sensing of Environment*, **94**, pp. 105–122.